

Time-Dependent Fracture Mechanics Considerations in Titanium 6Al-2Sn-4Zr-6Mo at Elevated Temperatures

D. E. Mills¹, T.S. Cook¹
¹Rolls-Royce, Indianapolis, USA

1 INTRODUCTION

Understanding of time-dependent crack growth stems from the mechanism map [1], which has previously been available only for nickel-base alloys. Advanced aircraft gas turbine engines seek higher performance through increased thrust-to-weight ratios thus requiring similar understanding for titanium alloys. This paper discusses observations from high temperature fatigue crack growth testing of Titanium 6Al-2Sn-4Zr-6Mo. This effort to describe the time-dependent mechanisms includes development of a crack growth mechanism map.

Additionally, the contributing factors behind this mechanism map were investigated. Results of specimens with long dwell periods did demonstrate a change in growth rate. A change in appearance was observed on the fracture surfaces of the dwell specimens. The change in growth rate and the change in fracture surface do not trend with K_{max} as has been proposed for some nickel alloys [2]. The increase in growth rate was more closely related to the maximum applied load. Transition to a time-dependent mechanism, then, is attributed to increased creep deformation. Therefore, a model was developed to account for creep interaction on titanium crack growth rates in the time-dependent regime that is a function of maximum stress rather than maximum stress intensity.

2 MATERIAL DESCRIPTION

The titanium alloy used in this study was 6Al-2Sn-4Zr-6Mo, similar to AMS4981, an alloy commonly used in intermediate-temperature sections of gas turbine engines [3]. The properties of this alloy are influenced by its thermomechanical history [4]. Ti6246 is a solid-solution-strengthened alloy that responds to heat treatment as a result of the beta-stabilizing effect of its 6% molybdenum content [3]. Beta-forged material contains the best combination of good low-cycle fatigue and fatigue-crack growth resistance [4]. The material used in this study was triple melted and β -forged. The microstructure was characterized by a transformed β matrix with dispersed α laths. This microstructure displayed the expected Widmanstatten structure. Figure 1 illustrates the microstructure of the material tested and shows the mixture of finely dispersed and coarse α lath structures.

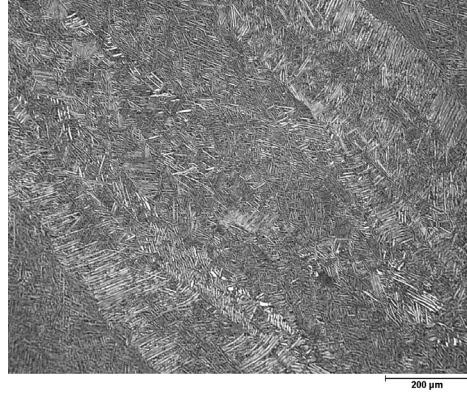


Figure 1. Ti6246 Microstructure

3 EXPERIMENTAL METHODS

Research previously conducted on titanium, albeit at lower temperatures and shorter dwell periods, did not demonstrate any noticeable change in fatigue crack growth rate when the specimen was subjected to dwell. The initial concept behind this test program was an examination of whether time-dependent mechanisms could be observed if the temperature was elevated beyond the typical application range for a given titanium alloy.

Fatigue crack propagation testing conducted at 510°C included hold times ranging from 1 to 900 seconds. Corner crack specimens were cut from a single disk forging. The specimens were oriented such that loading would be in the circumferential direction with crack propagation in the radial direction (C-R load - crack orientation). Specimen blanks were produced at multiple radial positions. Loading was based on a predominantly trapezoidal waveform with 1 second ramps for loading and unloading. The dwell period at maximum load ranged from 1 second to 900 seconds. The minimum load period was 1 second throughout the program. Tests were conducted at two levels of mean stress, either $R = 0.05$ or $R = 0.50$. Testing was conducted by Westmoreland Mechanical Testing & Research, Inc. using a constant maximum load. An illustration of the loading profile is provided in Figure 2.

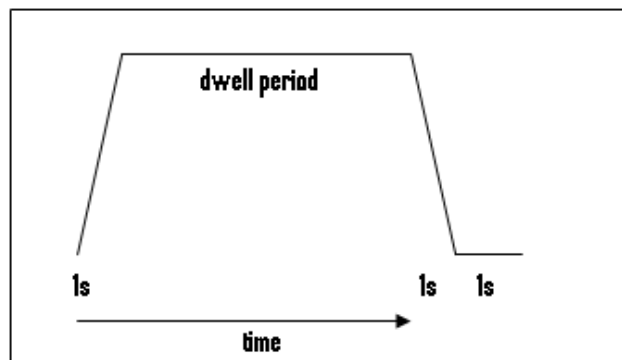


Figure 2. Test Cycle Profile, 1-h_t-1-1

All tests, except one, were conducted using a single maximum load for the entire test. In one test, the load was raised to determine the effect of changing the stress ratio. In addition, baseline tests were conducted using a sinusoidal waveform. These coupons were run at a frequency of 0.25 Hz, the same as the trapezoidal wave. These tests were run at stress ratios of both 0.05 and 0.5.

4 RESULTS AND DISCUSSION

The results of the testing are summarized in the crack growth plot shown in Figure 3. The baseline test results showed no difference between the two different wave forms at 0.25 Hertz. One striking observation is that at the low R-ratio, the hold time had no effect except for the longest hold at 900 seconds. This single test produced an acceleration of approximately 3x in growth rate over the data covering 0.25 to 0.0033 Hz. It was this failure to demonstrate a role of K_{max} for this mean stress that suggested a need for a different model.

Close examination of the $R = 0.5$ data illustrated that the dwell specimens did not show a consistent result. The baseline data at 0.25 Hz was not affected by the wave shape and was in agreement with the $R = 0.05$ result, although the higher stress ratio was slightly faster than the $R = 0.05$ curve. The growth increased, as expected, with the 120-, 300-, and 900-second hold time for the majority of tests. However, duplicate coupons with a 300-second hold showed one coupon had a 5x faster growth rate than the second coupon. Two of the three 900-second hold time curves were in good agreement, but the third test, over a small growth regime, displayed a much faster growth rate. The latter data was procured from the multiple R-ratio test. Despite the lack of agreement among the various tests, the increase in growth rate in the $R = 0.5$ data at conditions where no increase was observed at $R = 0.05$ clearly omits the expected K_{max} model from being considered.

The two 900-second hold bars were run at two different stress levels. The initial slopes of the growth rate curves are similar, but the higher maximum stress curve turns upward and has a slope similar to the third 900-second hold result, also tested at the high maximum stress. The change in slope occurs at a rate similar to the rate of decrease of the remaining area.

Observing that the maximum load was substantially higher for many of the high stress ratio tests, a simple creep evaluation was conducted on the specimens. The increase in growth rate appeared to be predictable based on this simple calculation. This simple calculation did not account for an increase in creep strain as the remaining section was reduced due to crack advancement. This consideration may also explain the change in slope previously observed.

da/dN vs. ΔK Graph

Material : TI 6246 Environment : Lab Air
 Temperature : 510°C Frequency : noted

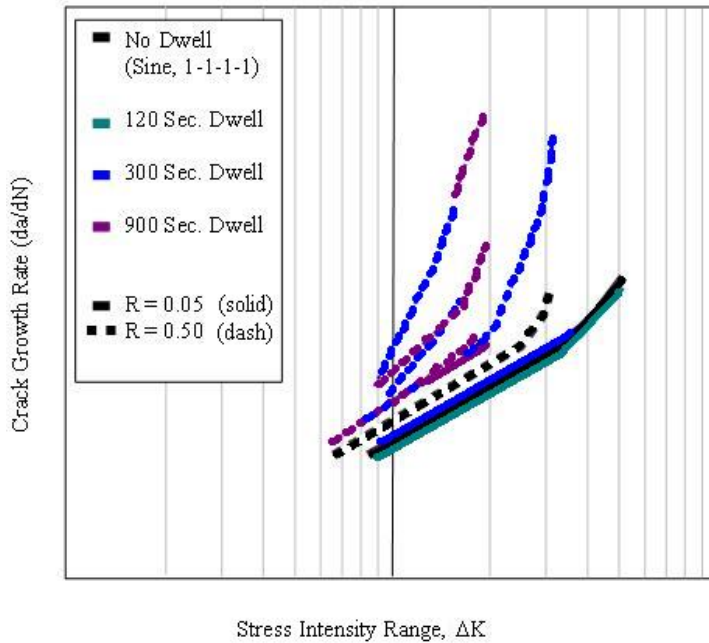


Figure 3. Growth Rate Results

An additional R = 0.50 specimen was tested with a lower applied load. The results from that specimen lined up with the R = 0.05 results. Since the two specimens had similar maximum load and test durations, creep estimates were very similar, ruling out a simple stress ratio effect.

A cyclic crack growth rate model, derived from the 1-second dwell baseline data, was incorporated into a life estimation using the crack growth code DARWIN™. The ratio of the actual life *versus* predicted (A/P) life for each specimen was plotted against the estimated creep strain in Figure 4.

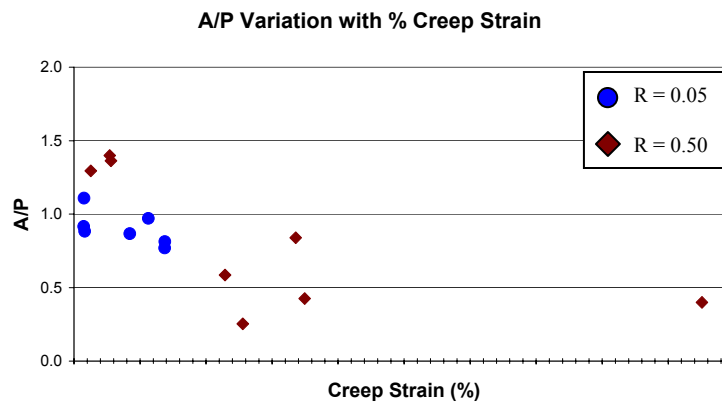


Figure 4. A/P Comparison to Creep Strain

When minimal creep was present in the material, the fatigue crack growth rate was more or less time independent. As the creep increased, the crack progression rate increased. There appeared to be a limit strain below which the growth process was purely cyclic. Metallurgical examination of the fracture surfaces confirmed the mechanism transition. The fracture surface in Figure 5a and 6a appears as expected for Ti6246. The surface is only slightly textured, and shows indications of ductile striations throughout the crack propagation. The remainder of Figures 5 and 6 provides a view of the effect of increase in creep strain on the fracture surface. The transition in the fracture surface is evident. The surface becomes increasingly textured and there is no clear evidence of striations on the surface. The crack growth becomes increasingly intergranular in nature. The trend is much less obvious on the $R = 0.05$ specimens, but it is visible to a limited degree in Figure 7. This comparison was made for 1-1-1-1 and 1-900-1-1 loading. The 5-minute dwell test showed the beginning of the transitional fracture surface. The creep from this specimen was much less than that of the $R = 0.5$ specimens due to load and test duration.

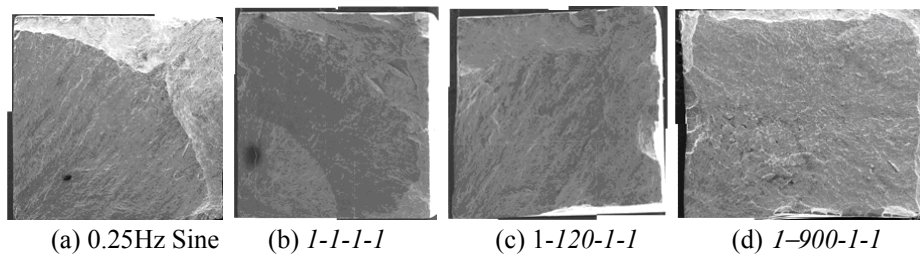


Figure 5. Fracture Surfaces for $R = 0.50$ Specimen

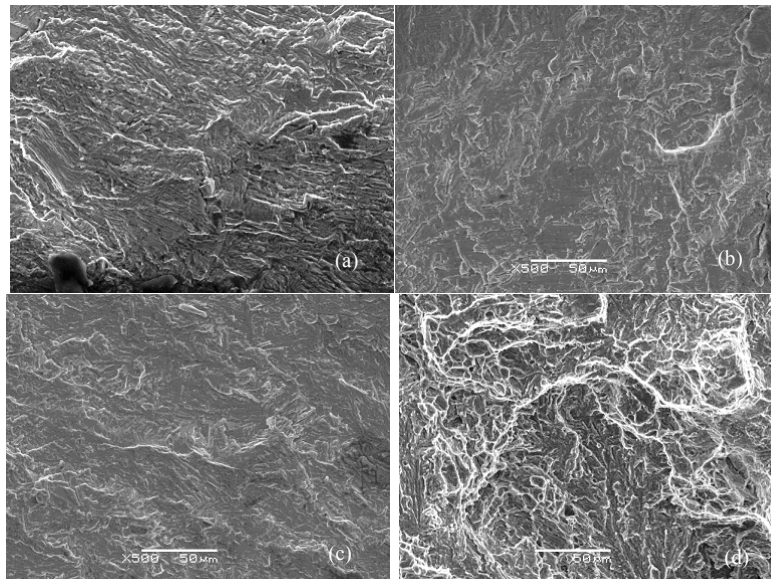
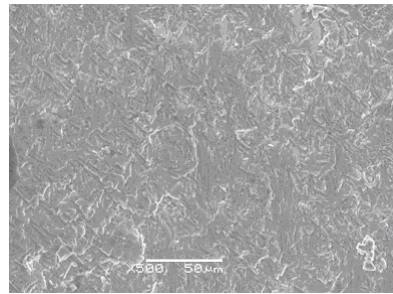
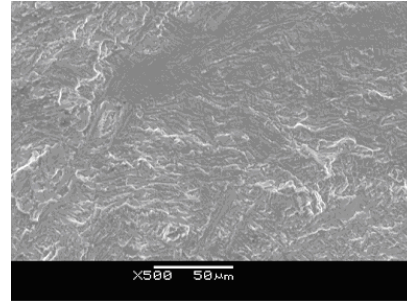


Figure 6. SEM Photomicrographs of $R = 0.50$ Fracture Surfaces

(a) 0.25Hz Sine, 0.13% ϵ creep (b) 1-1-1-1, 0.27% ϵ creep,
(c) 1-120-1-1, 1.68% ϵ creep, (d) 1-900-1-1, 4.75% ϵ creep



1-1-1-1



1-900-1-1

Figure 7. SEM Photomicrographs of $R = 0.05$ Fracture Surfaces

4.1 Mechanism Map

The concept of the mechanism map has been successfully used to describe the transition of other alloys from cyclic crack growth to time-dependent crack growth. The work by Solomon and Coffin [1] introduced the nomenclature of a *cyclic*, *mixed*, and *time-dependent* regime of fatigue crack growth. In the current study, these terms are used to define the regions where the growth is fully cycle dependent, where creep begins to influence the crack growth rate, and where the creep behavior dominates the observed crack growth behavior, respectively.

4.1.1 Cyclic Regime

Cyclic crack growth behavior is observed when there is minimal creep strain in the specimen. Crack growth rates are independent of dwell periods. The fracture surfaces do not demonstrate texturing or localized creep effects. The rate of crack progression can be modeled using standard linear elastic fracture mechanics models and assumptions.

4.1.2 Mixed (Transitional) Regime

Both time-dependent and cyclic mechanisms contribute to the total propagation rate. Fracture surfaces begin to demonstrate texturing associated with time-dependent growth, but ductile striations are still somewhat visible on the fracture surface. The crack growth becomes increasingly intergranular in nature. The influence of the time-dependent mechanism on growth rate is increasing. At the transition to this region, the resulting crack growth rate is only slightly elevated from that of similar conditions in the cyclic regime.

This regime presents an interesting phenomenon, though. When the specimen was on the mostly cyclic end of this regime, creep relaxation was possible. When specimen loading was sufficiently low, some drop off in crack growth was observed. Figure 8a illustrates the crack length *versus* cycles plot from one of the specimens with a lower applied load. The cyclic-only data clearly did not provide the correct estimate of the growth rate, but the apparent shapes of these two plots indicate that some level of relaxation was taking place at the larger crack lengths – a point at which acceleration would normally be expected.

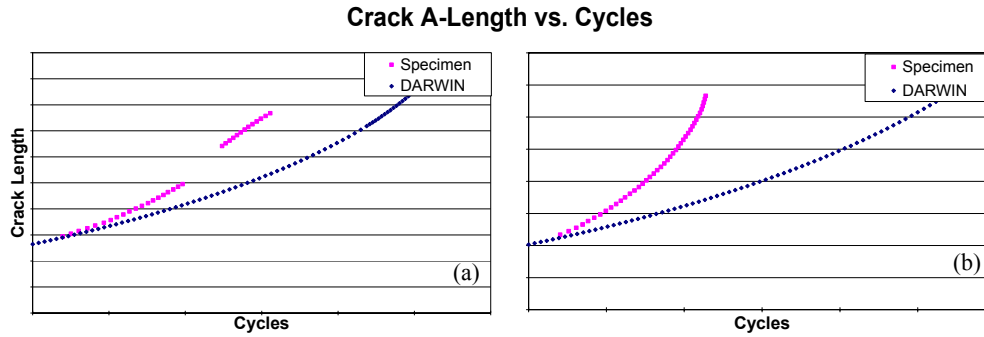


Figure 8. Crack Length vs. Cycles for $R = 0.5$, 900s Dwell Specimen
 (a) Low Applied Load, (b) High Applied Load

Other titanium crack growth research provides alternative views of the crack growth mechanism at work in this regime. Lesterlin *et.al.* [5] observed that the dwell response of Ti6246 was due to environmental influences rather than creep. Evans [6] observed that the change in growth rate was largely due to oxidation. Results from this study do not attempt to refute the claims made by Lesterlin or Evans. The goal, rather, is to explain the observed increase in crack growth rate with consideration that multiple mechanisms could be interacting on the crack front within this regime.

4.1.3 Time-Dependent (Creep Interaction) Regime

The time required to grow a crack a specific distance is a function of its cyclic loading and the creep deformation. Fracture surfaces are extremely textured and do not demonstrate evidence of ductile striations. Crack growth is largely intergranular in nature. Growth rates vary widely, but show a dramatic increase over baseline, no dwell tests. Figure 8b shows the cycle versus crack length for a duplicate specimen to the one represented in Figure 8a. The only difference was the applied load, which was 60% higher. The percent creep strain in this specimen was the largest of any tested.

Based on the creep strain of the specimen, the mechanism map can be illustrated in terms of the increase in growth rate expected (see Figure 9).

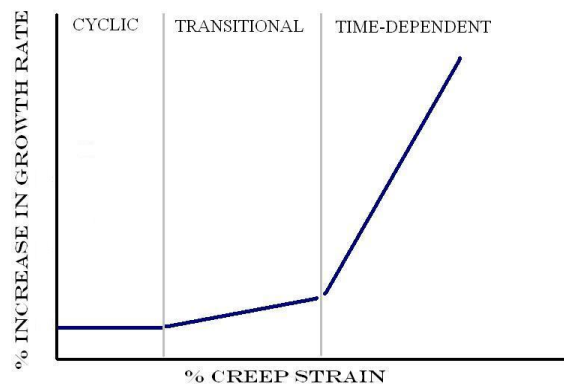


Figure 9. Mechanism Map for Ti6246

4.2 Time-Dependent Crack Growth Relationship

The mechanism map has been defined in terms of percent creep strain. The description of the regimes included how that mechanism developed with respect to the observed growth rate and fracture surface. Therefore, it is now possible to define a relationship for analytical predictions of crack growth life. The assertion from these results is that time-dependent crack growth in titanium alloys can be modeled as proportional to the creep strain, and thus influenced by the duration of hold time at a given σ_{\max} .

Creep models based on specimen testing plot stress for a given creep strain versus the exposure time. Using this approach, a superposition model can be defined that considers the total growth from a given cycle as the sum of the cyclic contribution and the interaction of creep deformation. Figure 10 provides the results of four specimens to illustrate this method.

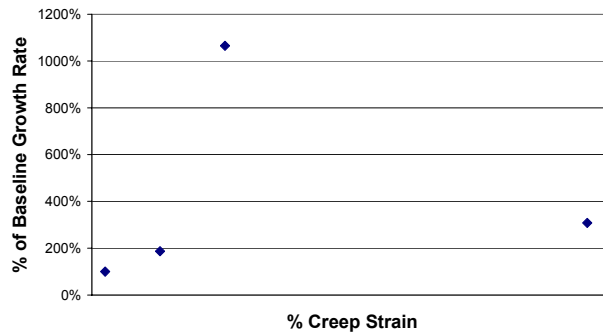


Figure 10. Increase in Growth Rate Based on Creep Strain

The work of Lesterlin [5] and Evans [6] indicates that additional considerations are needed to account for the influence of environment. The trend from Figure 10 supports the concept that additional mechanisms are interacting within the transitional regime. The testing within this program was not sufficient to separate these mechanisms. The total relationship for growth, though, should be written in the following form to include this consideration:

$$\Delta a \text{ per cycle} = \Delta a_{\text{cyclic}} + \Delta a_{\text{creep}} + \Delta a_{\text{environment}} \quad (1)$$

The cyclic growth from Equation 1 is calculated using linear elastic fracture mechanics with an applicable growth rate relationship (da/dN_c) for the given temperature. The time-dependent terms are determined experimentally. The relationship for Δa_{creep} would include terms for time and maximum stress for a given temperature, incorporating the preferred model from creep strain testing. Therefore, substituting these concepts into Equation 1, the superposition model could be expressed as:

$$\frac{da}{dN}_{perCycle} = \frac{da}{dN}_c + \Delta \frac{da}{dN} F^n(\sigma_{MAX}, \Delta t) + \Delta \frac{da}{dN}_{environment} \quad (2)$$

Equation 2 is illustrated in Figure 11 with respect to how various testing provides the basis for each term in the equation. The current research only included laboratory air and dwell data. Therefore, the actual level of separation between these curves is still being quantified. To provide a more accurate account for the observed increase in growth rate, vacuum testing would be needed. Additional work is currently planned and funded by Rolls-Royce.

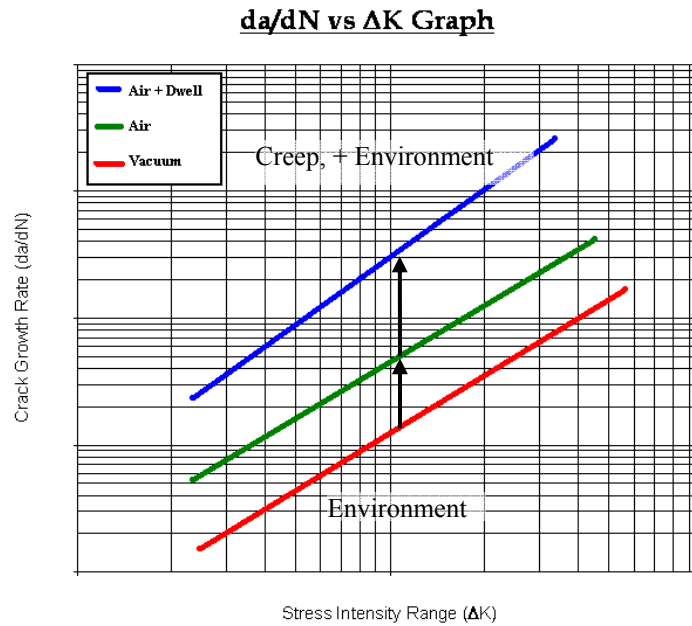


Figure 11. Illustration of Testing for Time-Dependent Relationship

5 CONCLUDING REMARKS

The results of this dwell testing program provide some interesting observations. The dwell time alone was not sufficient to create an increase in crack growth rate. Once time-dependent crack growth was observed, many of the specimens showed a nonlinear crack growth rate. The nonlinear behavior was suspected to be related to an increase in creep strain as the ligament decreases during crack propagation rather than the beginning of stage III crack growth. The results provide the following foundation from which to based future work on this topic:

- A mechanism map can be defined for time-dependent crack growth in titanium
- The transition to time-dependent crack growth is dominated by percent creep strain rather than the K_{max} – dwell time model expected for nickel alloys
- Additional testing is needed to quantify the environmental influence

6 REFERENCES

1. H.D. Solomon and L.F. Coffin, Jr, "Effects of Frequency and Environment on Fatigue Crack Growth in A286 at 1100 F," *Fatigue at Elevated Temperatures*, ASTM STP 52, American Society for Testing and Materials, 1973, pp. 112-122
2. R.H. Van Stone and D.C. Slavik, "Prediction of Time Dependent Crack Growth with Retardation Effects in Nickel Base Alloys," *Fatigue and Fracture Mechanics, 31st Volume*, ASTM STP 1389, American Society for Testing and Materials, 2000, pp. 405-426
3. *Materials Properties Handbook: Titanium Alloys*, AMS International, 1994, p 465
4. Titanium Metals Corporation (TIMET), www.timet.com, Technical Data Sheets: TIMETAL® 6-2-4-6, copied October 2008
5. S. Lesterlin, C. Sarrazin-Baudoux, and J. Petit, "Temperature-environment interactions on fatigue behaviour in Ti 6246 alloy", in: *Titanium '95: Science and Technology*, proceedings of the Eighth World Conference on Titanium, 1996, pp. 1211-1218
6. W. J. Evans, "Time dependent effects in fatigue of titanium and nickel alloys," *Fatigue Frac Engng Mater Struct*, 27, 2004, pp543-557